International Journal of Pharmaceutics: X 9 (2025) 100325

Contents lists available at ScienceDirect

International Journal of Pharmaceutics: X

journal homepage: www.sciencedirect.com/journal/international-journal-of-pharmaceutics-x

Fucoidan/Polyvinylpyrrolidone/Hesperitin nanoparticle complex for corneal injury treatment: Synthesis, characterization, and therapeutic efficacy

Yalu Liu [a,b,c], Zhengpei Zhang [a,b,c], Lina Guan [a,b,c], Jie Li [a,b,c], Xing Ge [a,b,c], Xiaochen Wu [d,**], Haiyang Liu [a,b,c,*]

[a] The Affiliated Xuzhou Municipal Hospital of Xuzhou Medical University, Xuzhou 221002, China
[b] Department of Ophthalmology, Xuzhou First People's Hospital, Xuzhou 221002, China
[c] Eye Disease Prevention and Treatment Institute of Xuzhou, Xuzhou 221002, China
[d] College of Chemical Engineering, Qingdao University of Science and Technology, Qingdao 266042, China

ARTICLE INFO

Keywords:
Fucoidan
Polyvinylpyrrolidone
Hesperitin
Corneal repair

ABSTRACT

Corneal injury is a common ailment that, if not addressed promptly and efficiently, has the potential to result in significant visual impairment. This study investigates the therapeutic potential of a novel FU/PVP/Hes nanoparticle complex composed of fucoidan (FU), polyvinylpyrrolidone (PVP), and hesperitin (Hes) for corneal injury treatment. The FU/PVP/Hes nanoparticles were synthesized using a solvent evaporation method and characterized for their morphology, size distribution, biocompatibility, antioxidant activity, and anti-inflammatory capacity. The nanoparticles demonstrated excellent biocompatibility with low hemolysis rates and minimal cytotoxicity. They also exhibited potent antioxidant and anti-inflammatory properties, which were attributed to the enhanced solubility and bioavailability of Hes through nanoparticle formation. *In vivo* investigations employing a mouse model of corneal injury induced by alkali burns showed that the FU/PVP/Hes nanoparticles significantly promoted corneal epithelial healing, reduced corneal opacity, and suppressed the elevation of inflammatory cytokines. Histopathological analysis confirmed the nanoparticles' ability to facilitate corneal tissue repair. The study concludes that the FU/PVP/Hes nanoparticle complex is a promising therapeutic agent for corneal injury treatment due to its biocompatibility and multifaceted therapeutic effects.

1. Introduction

Corneal injury refers to damage to the transparent corneal tissue of the eye caused by external factors or infection. It may occur in everyday scenarios such as accidental injury, improper use of contact lenses, or eye surgery.(Barrientez et al., 2019; Liu et al., 2023) The severity of corneal injuries depends on the depth and extent of the damage. Mild injuries can cause eye pain and discomfort, while severe injuries can affect vision and lead to infections. Improper or delayed treatment of corneal injuries can result in serious consequences, including bacterial or fungal infections, corneal scarring, vision impairment, or even permanent vision loss.(Griffith et al., 2017; Yu et al., 2024) The accompanying persistent pain and discomfort can prolong the recovery time and impact the patients' daily activities and work. Therefore, timely medical attention and appropriate treatment are crucial in addressing corneal injuries to prevent and alleviate the potential serious consequences.(Ger et al., 2023; Yang et al., 2023b).

Commonly used treatment medications include antibiotic eye drops for preventing and treating infections, artificial tears for lubrication, anti-inflammatory drugs to reduce inflammation, and corneal repair medications to promote healing. (Dang et al., 2022) Severe corneal injuries may require surgical treatment, such as corneal transplant surgery to repair damaged corneal tissue.(Chen et al., 2018) Hesperitin (Hes) is a naturally occurring bioflavonoid found in citrus fruit peels and other plants, known for its antioxidant and anti-inflammatory properties.(Cao et al., 2022; Li and Schluesener, 2017) However, Hes shows poor solubility in aqueous solution, which limit its speed and extent to reach therapeutic concentrations, ultimately reducing its efficacy.(Jiang et al.,

* Corresponding author at: The Affiliated Xuzhou Municipal Hospital of Xuzhou Medical University, Xuzhou 221002, China.
** Corresponding author.
E-mail addresses: wxcguest@126.com (X. Wu), liuhaiyang86@126.com (H. Liu).

https://doi.org/10.1016/j.ijpx.2025.100325
Received 8 December 2024; Received in revised form 23 February 2025; Accepted 25 February 2025
Available online 26 February 2025

2023) Multiple strategies are employed to address the issue of poor solubility. (Shen et al., 2015; Simao et al., 2020) For example, lipid nanocarriers loaded with Hes were prepared using the phase inversion temperature method, showing excellent *in vitro* cytotoxicity against glioblastoma cells.(Simao et al., 2020).

Fucoidan (FU), a sulfated polysaccharide found in various species of brown seaweed, has been studied for its potential applications as a drug carrier due to its biocompatibility, biodegradability, and therapeutic properties.(Tran et al., 2016; Zahariev et al., 2023) FU can form stable complexes with drugs through electrostatic interactions, enhancing the solubility, stability, and bioavailability of the drugs.(Han et al., 2022) Furthermore, FU exhibits a diverse array of biological functions, including anti-inflammatory, antioxidant, and antitumor effects, making it an appealing candidate for drug delivery systems.(Cardoso et al., 2016; Zahariev et al., 2023).

Polyvinylpyrrolidone (PVP) is a commonly used high-molecular-weight polymer material with excellent biocompatibility, often employed as a drug carrier. (Franco and De Marco, 2020; Mikayilov et al., 2024) PVP possesses outstanding solubility and biocompatibility, making it suitable for encapsulating and stabilizing drugs to enhance their solubility and bioavailability.(Manju and Sreenivasan, 2011; Yin et al., 2012) As a conventional drug carrier material, PVP can be prepared into different forms (such as nanoparticles, microparticles, *etc.*) through various methods to meet the requirements of different drugs and applications.(Adami et al., 2017; Zhou et al., 2024) Based on this, the study utilizes PVP and FU as carriers to load Hes, forming a FU/PVP/Hes nanoparticle complex for alleviating corneal damage. The morphology, structure, biocompatibility, and *in vivo* efficacy of the FU/PVP/Hes nanoparticles are thoroughly investigated.

2. Materials and methods

2.1. Materials

Hesperitin (Hes, > 97 %) was bought from Sigma-Aldrich Corp. Polyvinyl pyrrolidone (PVP-K17, molecule weight: 8000) was obtained from Dalian Meilun Biotechnology Co., Ltd. Fucoidan (FU) was procured from Shandong Jiejing Group Co., Ltd.

2.2. Preparation of FU/PVP/Hes nanoparticles

50 mg of polyvinylpyrrolidone (PVP) and 30 mg of hesperidin (Hes) were thoroughly dissolved in 1 mL of ethanol. Then the mixture was added dropwise to a 10 mL solution of 10 mg/mL fucoidan (FU), followed by vertexing for 2 h, rotary evaporation to remove ethanol, and obtained the FU/PVP/Hes nanoparticles.

2.3. Characterization

The morphology of the FU/PVP/Hes nanoparticles was characterized by a Transmission electron microscopy (TEM, JEM-2100F, Japan). Granulometric distribution of the FU/PVP/Hes nanoparticles was measured by a NanoBrook Omni (Brookhaven Instruments, Holtsville, New York).

2.4. Hemolysis

5 μL of the FU/PVP/Hes nanoparticles (1, 2, 5, 10, 20, 1000 μg/mL) was combined with 3.5 mL of a 0.9 % saline solution and 0.1 mL of anticoagulant blood. The blend was maintained at a temperature of 37 °C and allowed to incubate for a duration of 1 h, centrifuged, and the absorbance of the supernatant at 545 nm was measured by a HBS-ScanX microplate reader (Nan Jing DeTie Laboratory Equipment Co., Ltd.) to calculate the hemolysis. Hemolysis $= (A_s\text{-}A_-)/(A_+\text{-}A_-) \times 100$ %, wherein As denotes the absorbance of the FU/PVP/Hes complex, A_- represents the absorbance of the negative control, and A_+ indicates the absorbance of the positive control, respectively. The negative and positive controls were established by separately incubating 0.1 mL of anticoagulated blood with 3.5 mL of 0.9 % saline solution for the negative control, or with 3.5 mL of H_2O for the positive control, at 37 °C for 1 h.

2.5. Cytotoxicity

5 μL of the FU/PVP/Hes nanoparticles (1, 2, 5, 10, 20, 1000 μg/mL) was co-cultured with L929 cells at 37 °C for 24–72 h. Subsequently, cytotoxicity was measured by a standard MTT assay.

2.6. In vitro antioxidant activity

The antioxidant capacity of both Hes and the FU/PVP/Hes nanoparticles was assessed using the iron reduction antioxidant potential (FRAP) method. Three distinct solutions were acquired as follows: the first was a 0.3 M acetate buffer adjusted to a pH of 3.6, the second was a 0.01 M solution of 2,4,6-tripyridyltriazine diluted in 0.04 M HCl, and the third was a 0.02 M $FeCl_3$ solution prepared in PBS with a pH of 7.4. These solutions were combined in a volume ratio of 10:1:1 to create the working solution. Subsequently, 5 μL of Hes (6.25–100 μg/mL) or FU/PVP/Hes nanoparticles (37.5–600 μg/mL, containing Hes 6.25–100 μg/mL) was combined with 180 μL of the working solution within a 96-well plate, respectively. The absorbance of the solution at 593 nm was continuously monitored to track changes over time. The antioxidant capacity was quantified in terms of the concentration of the reaction product (Fe^{2+}, mM), utilizing a standard curve that was established from a solution of standard ferrous sulfate.

2.7. Intracellular anti-inflammatory capacity

The FU/PVP/Hes solution was diluted to a concentration of 60 μg/mL with the use of DMEM and subsequently sterilized for future use. RAW264.7 cells were plated in a 6-well plate at a seeding density of 400,000 cells per well. Following a 24-h incubation period at 37 °C, the culture medium was replaced, and the cells were treated with 2 mL of lipopolysaccharide (LPS, 1 μg/mL) for 2 h to induce cellular oxidative stress. Upon removal of the LPS solution, the cells were treated with 2 mL of the 60 μg/mL FU/PVP/Hes solution and further incubated for 16 h. Subsequently, the cellular morphology was examined using an Olympus CKX5 microscope, and total RNA was extracted using Trizol reagent for the analysis of the relative expression levels of TNF-α and IL-1β *via* RT-PCR.

2.8. In vivo treatment of alkali burns induced corneal injury

All animal experiments comply with the ARRIVE guidelines (Animal Research: Reporting of *In Vivo* Experiments) and were approved by the Ethics Committee for Animal Experimentation at Qingdao University of Science and Technology (QKDLL-2024-48). The right eyes of C57 mice, which were male, aged 7–8 weeks, and obtained from Qingdao Darenfucheng Animal Technology Co., Ltd. (Qingdao, China), were utilized in the experiments. These mice were deemed healthy and exhibited no observable ocular abnormalities.

The alkali burn model of the mouse cornea was established following a previously reported protocol.(Yin et al., 2021a; Yin et al., 2021b; Zhang et al., 2020) Prior to the procedure, the mice were rendered unconscious by administering a 4 % chloral hydrate solution through an intraperitoneal injection and received topical ocular anesthesia with 0.4 % oxybuprocaine hydrochloride eye drops. Under an optical microscope, the mice's eyelashes and excess hair around the eyes were trimmed, and the area around the mouse's eyeball was gently cleaned with a cotton swab soaked in saline solution. A filter paper (2 mm in diameter) was saturated in 1 M NaOH for 5 min, and then placed on the central cornea of the mice for 60 s to induce alkali-induced corneal injury.

Table 1
Scoring criteria of corneal opacity.

Score	Corneal condition
0	Clear, No opacity present
1	Hazy, Sparse or diffuse opacity, iris clearly visible
2	Semi-translucent area distinguishable, iris blurred
3	Greyish-white translucent area present, iris details unclear, pupil size barely visible
4	Opaque cornea, iris indiscernible

Subsequently, the eyes were washed with a 0.9 % saline solution for 10 s and immediately administered with 2 drops of the medication solution (~0.1 mL). The mice were divided into several specific groups as follows: the untreated control group, the group that was given Hes solution (3 mg/mL), the group that was given FU/PVP suspension (15 mg/mL), and the group that was given FU/PVP/Hes solution (18 mg/mL, containing 3 mg/mL of Hes). The medication drops were administered at a frequency of once every 24 h.

Using a slit lamp microscopy (YZ5X1, 66 Vision Tech Co., Ltd.), the eyes were examined at various time points following the alkali burns. The size of the epithelial defect was assessed and measured post-staining with 1.0 % sodium fluorescein. Corneal opacity scores on day 5 were determined according to an established methodology.(Kim et al., 2015; Wang et al., 2020) The grading of corneal opacity ranges from 0 to 4, with 4 being the highest score. The scoring criteria are as shown in the Table 1.

On the fifth day, the mice were sacrificed to extract their corneas and subjected to hematoxylin and eosin (H&E) staining to evaluate histopathological changes. The levels of specific cytokines (including vascular endothelial growth factor (VEGF) and interleukin-1β (IL-1β)) was quantitatively determined by RT-PCR.

2.9. Absorption of FU/PVP/Hes in the cornea

50 μL of Coumarin 6 (Cou-6, 1 mg/mL) was combined with 10 mL FU/PVP/Hes solution (15 mg/mL), and the blend was designated as FU/PVP/Hes/Cou-6. C57 mice were randomly assigned to two separate groups, with 5 μL of FU/PVP/Hes/Cou-6 or 5 μL of Cou-6 (5 μg/mL) being administered to the right eye, with each application separated by 10 min, for a total of three applications. Afterward, the mice were euthanized, and their eyeballs were extracted. The eyeballs were immersed in formaldehyde (4 %) for 1 h, and the corneas were then carefully dissected under a microscope. Following this, the corneas were leveled and then examined using a fluorescence microscope to document the uptake of Cou-6 within the corneal sections and photographs were taken.

2.10. Biosafety in vivo

Mice were given FU/PVP/Hes solution (18 mg/mL, containing 3 mg/mL Hes) twice a day for eye drops. On day 1 and day 7, the fluorescein fundus angiography of mice eye was examined using a fundus contrast machine (CRO Plus, Suzhou Weiqing Medical Equipment Co., Ltd).

The mice were continually given FU/PVP/Hes solution, weighted and record daily, and the weight changes was calculated by $\text{Weight change}\ (\%) = \frac{\text{Weight of mouse on Day } n}{\text{Weight of mouse on Day 1}} \times 100\%$.

On the 10th day, mice were euthanized. The spleen, liver, and kidneys were dissected and weighed to calculate organ indices: $\textit{Organ index}\ (\%) = \frac{\text{Organ weight}}{\text{Mouse body weight}} \times 100\%$

Pathological H&E staining was performed on the cornea, spleen, liver, and kidneys to observe the status of the organs.

2.11. Statistical analysis

The experiments were conducted in triplicate, and statistical significance was assessed by conducting a one-way analysis of variance (ANOVA), with statistical significance defined as a p-value less than 0.05.

3. Results and discussion

As shown in Fig. 1A, the obtained FU/PVP/Hes nanoparticles are uniformly sized, well-dispersed, without aggregation or agglomeration. Particle size analysis in Fig. 1B indicates a most frequent diameter of 27.7 nm (PDI = 0.142), with a narrow size distribution range. The uniform particle size distribution of FU/PVP/Hes nanoparticles promises several advantages. It reduces the likelihood of aggregation or sedimentation, thereby enhancing stability in various formulations and facilitating predictable absorption and distribution in biological systems. Additionally, minimizing size distribution variability decreases batch-to-batch variations, which improves reproducibility and reliability in therapeutic applications.

The biocompatibility of FU/PVP/Hes nanoparticles is evaluated through hemolysis testing and cytotoxicity assays.(Jian et al., 2017) First, hemolysis testing is crucial in the development of eye drops because it assesses the toxic effects of the drug on red blood cells. To prevent damage to ocular tissues caused by hemolytic substances, the hemolysis of FU/PVP/Hes nanoparticles is measured in Fig. 2A. Even at a high concentration of 1000 μg/mL, FU/PVP/Hes nanoparticles demonstrate a minimal hemolysis rate of less than 5 %, suggesting low toxicity to red blood cells. FU/PVP/Hes nanoparticles do not cause red blood cell rupture and show no risk of damage to ocular tissues, suggesting their safety when applied to ocular tissues.

Secondly, the Cytotoxicity of FU/PVP/Hes nanoparticles is assessed using a MTT assay. The results of co-culturing L929 cells with different concentrations of FU/PVP/Hes nanoparticles for 24 to 72 h in Fig. 2B indicate that FU/PVP/Hes nanoparticles at concentrations of 20 μg/mL and below do not affect normal cell growth, with cell viability remaining above 100 % and no significant difference when compared with the blank control group. However, FU/PVP/Hes nanoparticles with a concentration of 1000 μg/mL shows cell viability of 99 %, 90 %, and 70 % at 24, 48, and 72 h, respectively, indicating minimal impact on cell viability within 48 h, but prolonged co-incubation for 72 h decreases cell viability. FU/PVP/Hes nanoparticles exhibits no cytotoxicity within a certain concentration range, but shows some toxicity at high

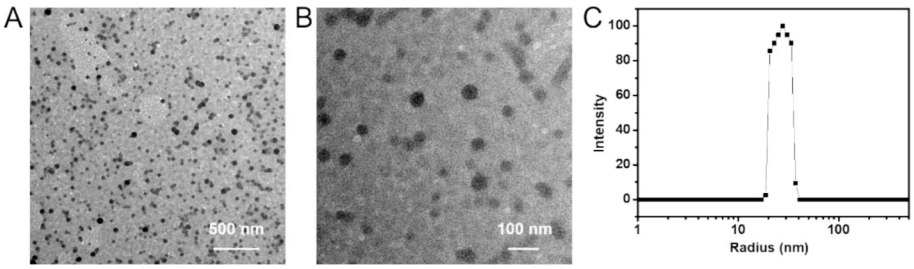

Fig. 1. (A-B) TEM images and (C) Granulometric distribution of FU/PVP/Hes nanoparticles.

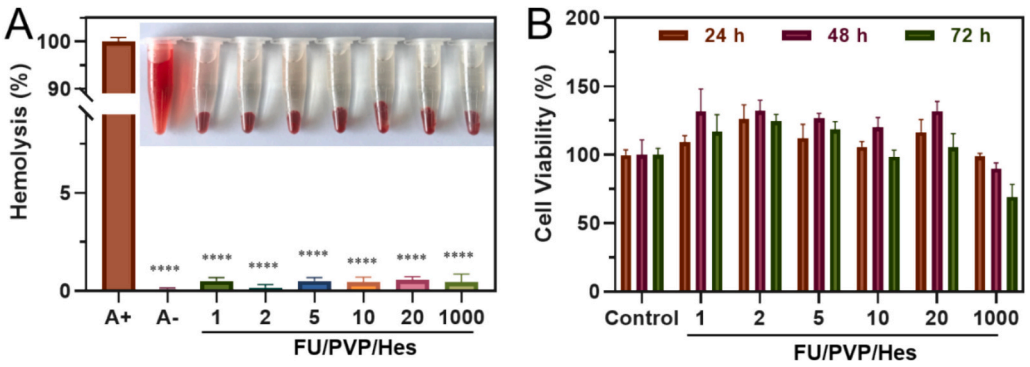

Fig. 2. (A) Hemolysis of FU/PVP/Hes, ****$p < 0.0001$ comparing to the A^+ group. A^-represented the negative control (0.9 % NaCl solution); A^+ represented the positive control (H_2O). (B) Cytotoxicity of FU/PVP/Hes. Number on the horizontal axis represents concentration of FU/PVP/Hes (1, 2, 5, 10, 20, 1000 μg/mL).

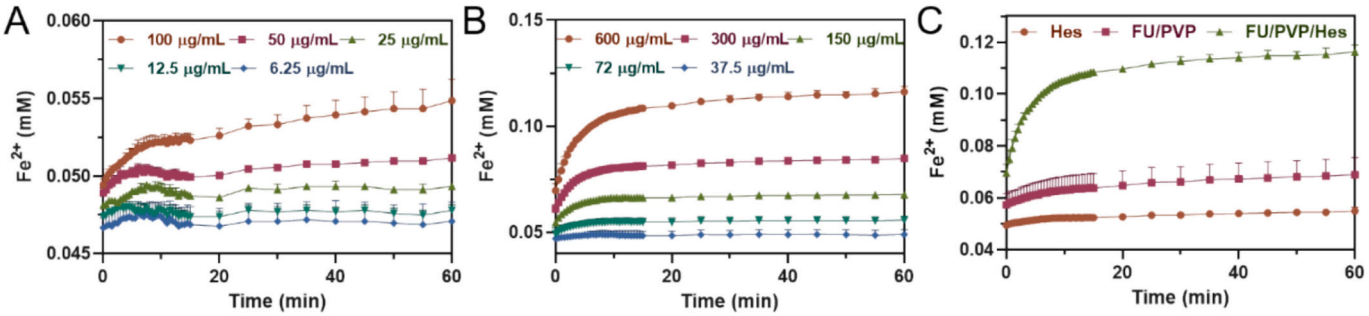

Fig. 3. *In vitro* antioxidant activity of Hes and FU/PVP/Hes on the kinetics of FRAP. (A) With different concentrations of Hes, (B) with different concentrations of FU/PVP/Hes, (C) with 0.1 mg/mL of Hes, FU/PVP and FU/PVP/Hes.

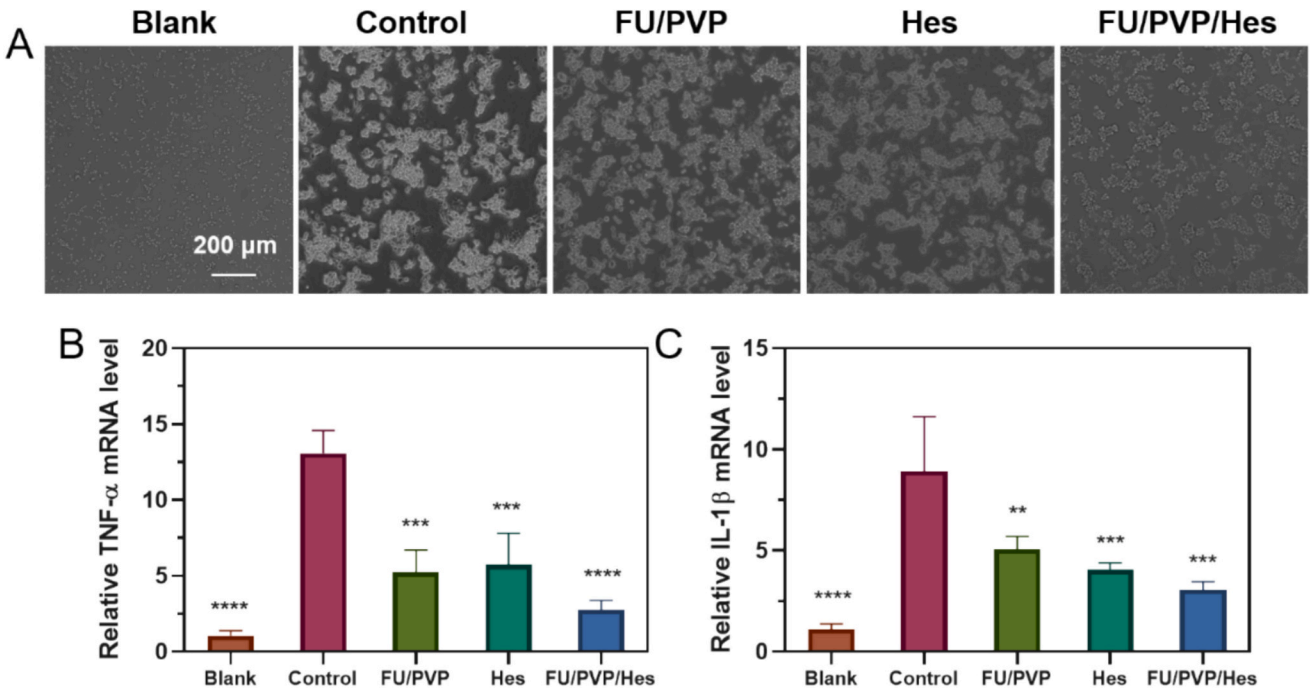

Fig. 4. (A) Cellular morphology of RAW264.7 cells after LPS stimulation and different treatments. (B-C) Secretion of (B) TNF-α and (C) IL-1β after LPS stimulation and different treatments. **$p < 0.01$, ***$p < 0.001$ and ****$p < 0.0001$ comparing to the control group.

concentrations (*i.e.*, 1000 μg/mL).

Hes is a flavonoid compound known for its strong antioxidant capabilities, which assist in neutralizing free radicals and safeguarding cells against oxidative stress. Similarly, FU also exhibits antioxidant activity. This antioxidant effect allows both Hes and FU to be widely utilized in health supplements and drug development, aiming to maintain the health of cells and tissues. As depicted in Fig. 3A using the FRAP assay, Hes exhibits antioxidative activity that correlates positively with

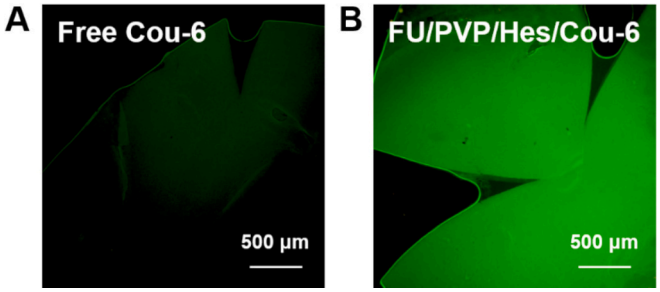

Fig. 5. (A-B) Fluorescence intensity of mouse cornea treated by (A) free Cou-6 and (B) FU/PVP/Hes/Cou-6.

its concentration. Higher concentrations typically result in stronger antioxidative effects because more Hes molecules can react with and neutralize free radicals, thus reducing the occurrence of oxidative damage. FU/PVP/Hes retains Hes's antioxidative activity and exhibits a concentration-dependent antioxidative effect similar to Hes alone (Fig. 3B). Moreover, at equivalent concentrations, FU/PVP/Hes shows higher antioxidative activity than both Hes alone and FU/PVP separately (Fig. 3C). This suggests that the formation of nanoparticles aids in the uniform dispersion of Hes in the aqueous solution, thereby enhancing overall antioxidative activity.

On the other hand, both Hes and FU possess anti-inflammatory activity, which is primarily attributed to their multiple regulatory effects on inflammatory pathways. Both are considered potential anti-inflammatory agents with promising therapeutic effects for inflammatory diseases. To evaluate the anti-inflammatory activity of FU/PVP/Hes, an LPS-stimulated cell model was utilized (Fig. 4). Following LPS stimulation, RAW264.7 cells typically display an inflammatory response. LPS, a potent immune stimulant, activates Toll-like receptor 4 (TLR4) on RAW264.7 cells, thereby initiating inflammation-related signaling pathways. This activation can induce the expression of inflammatory cytokines such as TNF-α and IL-1β, promoting the inflammatory response. As shown in Fig. 4A, RAW264.7 cells undergo a transformation from a relatively oval shape to a more irregular form, accompanied by an enlargement attributed to increased cytokine synthesis. The introduction of FU/PVP/Hes can partially improve the changes in cell morphology and alleviate cellular swelling. Moreover, the abnormal elevation of inflammatory cytokines particularly TNF-α and IL-1β can be effectively suppressed by FU/PVP/Hes (Fig. 4B & C). FU/PVP/Hes exhibits excellent antioxidant and anti-inflammatory capabilities, highlighting its potential therapeutic benefits in combating oxidative stress-related inflammatory conditions.

Based on the results of the above experiment, the reparative effect of FU/PVP/Hes on corneal alkali burns is studied. Before that, the absorption of FU/PVP/Hes on normal mouse corneas was tested (Fig. 5). FU/PVP/Hes is conjugated with Cou-6 and applied to the mice corneal

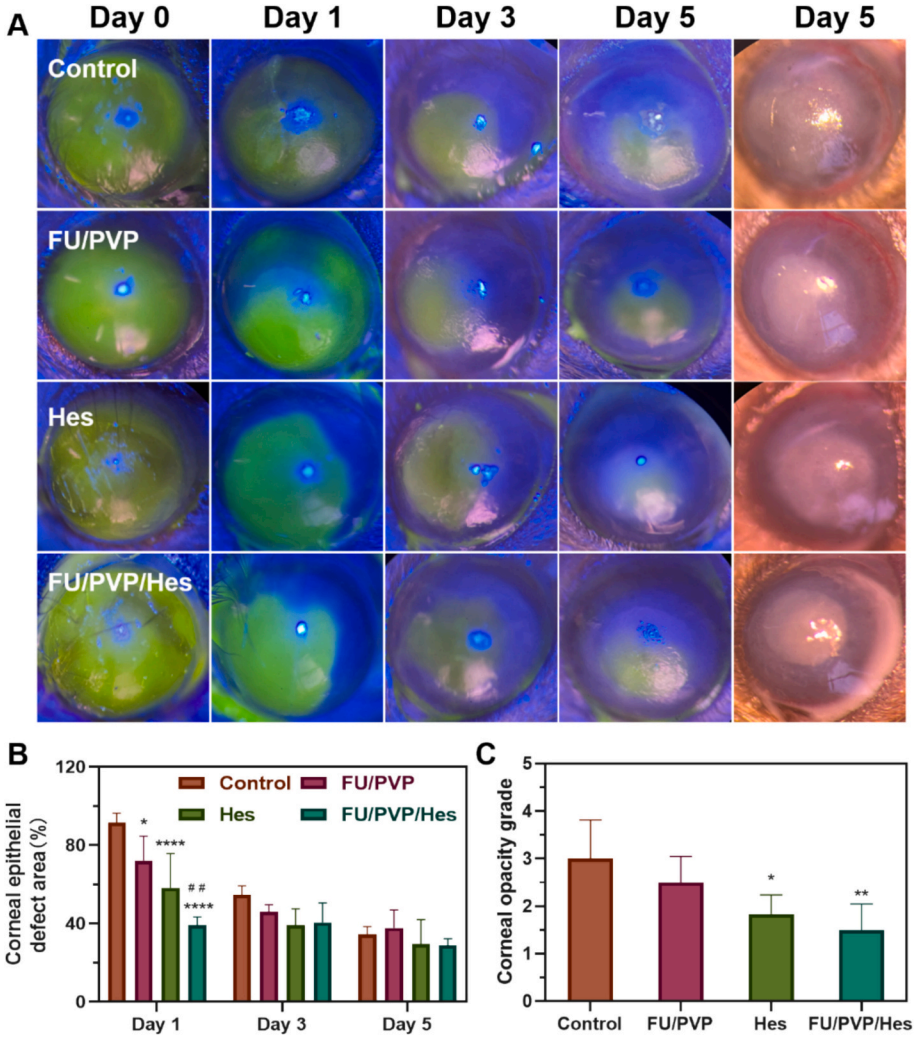

Fig. 6. (A) Fluorescent and optical photos of mice eyes after alkali burns under different treatments. (B) Percentage of corneal epithelial defect area remained on day 1, 3 & 5 in (A). (C) Corneal opacity grade on day 5. *$p < 0.05$ and ****$p < 0.0001$ comparing to the control group, ##$p < 0.01$ comparing to the FU/PVP group.

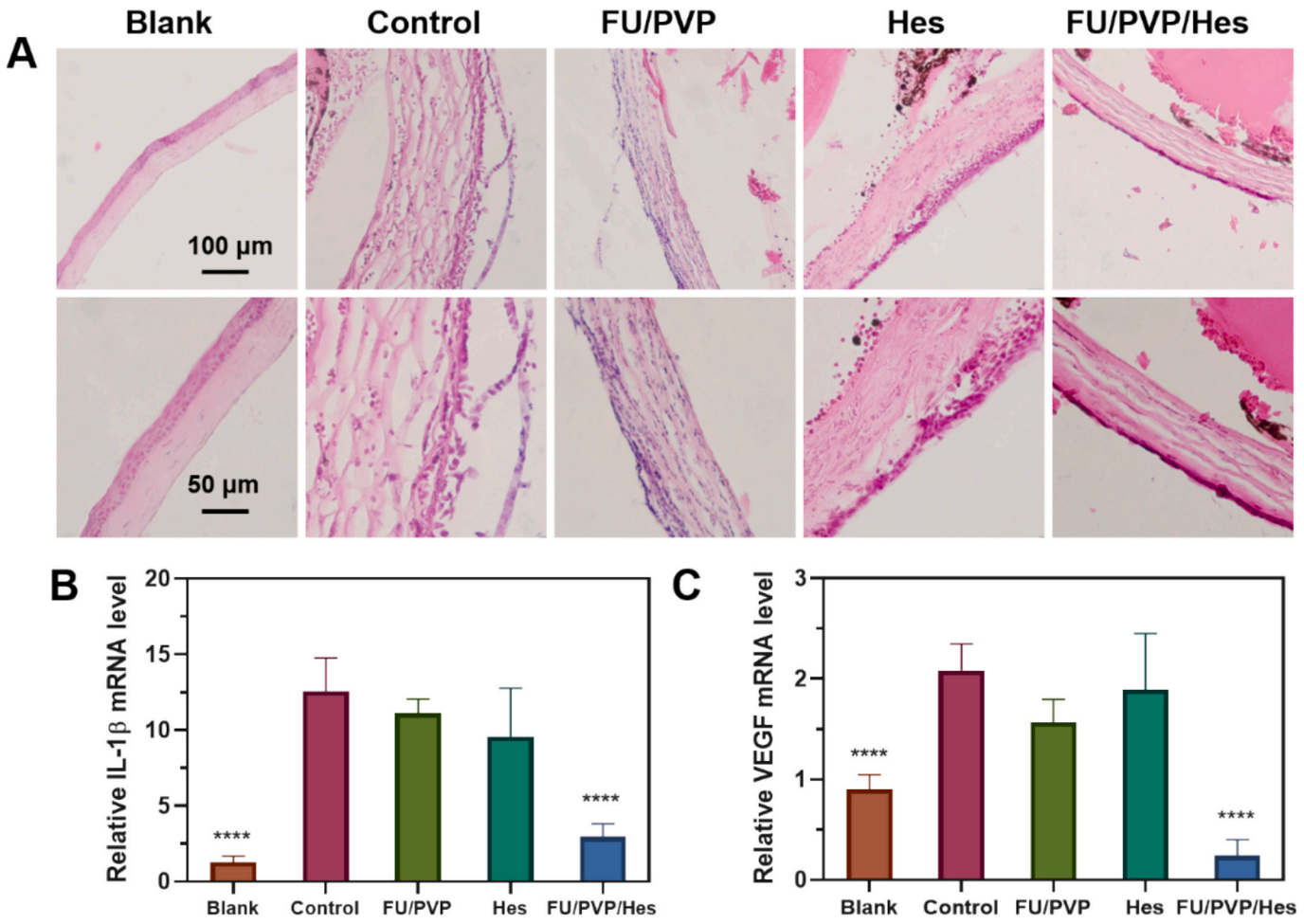

Fig. 7. (A) H&E staining histopathological evaluations of mice corneas on day 5. (B-C) Relative (B) IL-1β and (C) VEGF mRNA level on day 5. *p < 0.05, **p < 0.01 and ****p < 0.0001 comparing to the control group.

surface, after which samples are taken from the cornea and Cou-6 levels are measured and quantified using fluorescence microscopy. Cou-6 is an important fluorescent probe commonly used for *in vivo* tracking, cellular uptake, and transport mechanism research of drug delivery systems. By adsorbing Cou-6 onto FU/PVP/Hes nanoparticles, FU/PVP/Hes/Cou-6 nanoparticles with Cou-6 fluorescence can be obtained, which allows to characterize the adsorption amount of FU/PVP/Hes nanoparticles on the cornea through fluorescence intensity. The low fluorescence of Cou-6 alone on the cornea indicates its low adsorption capacity on the cornea (Fig. 5A). Under the same conditions, the fluorescence of FU/PVP/Hes/Cou-6 nanoparticles on the cornea is high (Fig. 5B), indicating that the absorption of FU/PVP/Hes/Cou-6 nanoparticles on the cornea is very high, which facilitates the efficacy of the nanoparticles.

To induce corneal burns, the mice corneas were treated with NaOH solution and then administered with drugs like FU/PVP/Hes. As shown in Fig. 6A, under cobalt blue light, all groups of mouse corneas exhibited fluorescent green staining after fluorescein sodium dyeing, indicating that the entire corneal epithelium was successfully eroded by NaOH. FU/PVP/Hes significantly promotes the recovery of corneal epithelial injuries, particularly in the early stages (the first day), which may be beneficial for the subsequent recovery of vision. In the control group as well as the group treated with FU/PVP, corneal healing was slow, with 34. 5 % and 37.8 % of the cornea unrepaired on the 5th day, respectively, whereas in the FU/PVP/Hes group, only 28.8 % of the cornea remained unrepaired (Fig. 6A & B). Corneal opacity score is a crucial indicator for assessing the efficacy of drugs in the mouse corneal alkali burn model. The scoring of corneal opacity integrates the conditions of the pupil, iris vessels, and anterior chamber tissues. Although some degree of corneal opacity was observed in all groups, corneas treated with FU/PVP/Hes showed significantly lower opacity *versus* the control group (Fig. 6C), indicating that FU/PVP/Hes effectively alleviates corneal opacity induced by alkali burns.

Histological examination of alkali-burned corneas provides a more definitive confirmation of clinical observations (Fig. 7A). In the control group as well as the FU/PVP treated group, corneas on the fifth day still exhibited significant inflammatory cell infiltration, with incomplete regeneration of the corneal epithelium. Corneas treated with Hes displayed uneven distribution of regenerated epithelial cells. Although incomplete epithelial regeneration was observed in all groups including the FU/PVP/Hes treated group, the corneal tissue treated with FU/PVP/Hes was most closely resembled that of the healthy mice in the blank group.

Moreover, similar to *in vitro* cell experiments, the anti-inflammatory and recovery-promoting effects of FU/PVP/Hes significantly suppress the abnormal elevation of inflammatory cytokine IL-1β level (Fig. 7B) in corneal tissue post-alkali burn, thereby reducing the risk of infection. In this way, FU/PVP/Hes may help effectively control pain, reduce swelling, and prevent further damage to the cornea. Additionally, FU/PVP/Hes can effectively inhibit the elevation of VEGF in the cornea after NaOH burns, which helps protect corneal structure and maintain visual function recovery (Fig. 7C). Excessive production of VEGF can lead to abnormal vascular leakage and inflammation, exacerbating the damage. The anti-inflammatory and anti-VEGF effects of FU/PVP/Hes emphasize its potential in treating complex eye diseases.(Ger et al., 2025; Ghosh

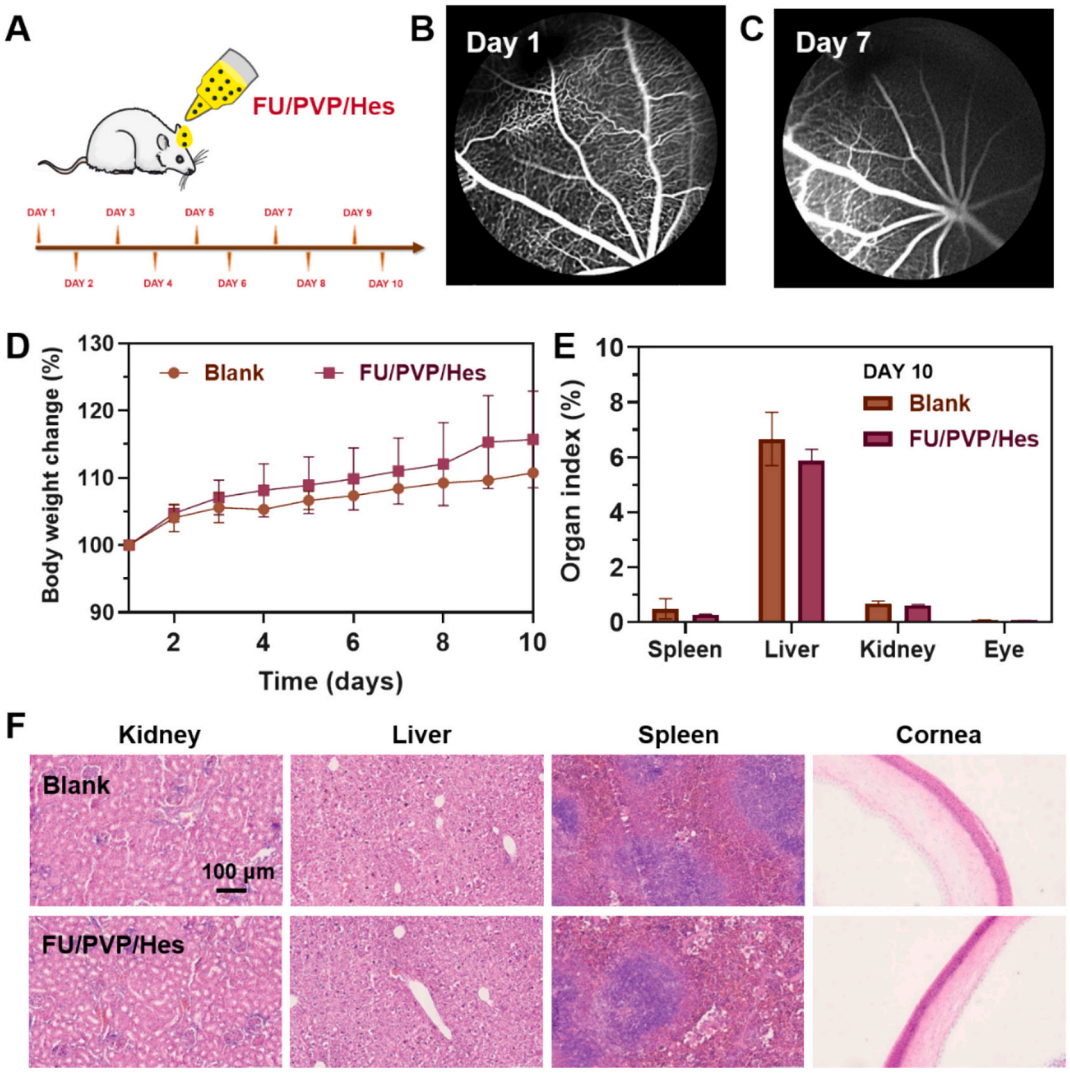

Fig. 8. Biosafety *in vivo*. (A) Experimental schematic diagram. (B-C) Fluorescein fundus angiography of mice eye after (A) 1 and (B) 7 days of FU/PVP/Hes administration. (D) Body weight change, (E) organ index, and (F) H&E staining histopathological evaluations of mice after given FU/PVP/Hes for 10 days.

et al., 2025; Luo et al., 2022; Yang et al., 2023a)

Furthermore, the *in vivo* safety of FU/PVP/Hes was preliminarily determined in Fig. 8. After continuous administration for 7 days, Fig. 8B & C showed that no visible lesions were observed in the fundi of mice through fundus imaging. After 10 days of continuous administration, it was found that the weight of the mice remained basically unchanged or slightly increased (Fig. 8D), with no downward trend, and the organ index showed no statistical difference compared to healthy mice in the blank group (Fig. 8E), indicating that the FU/PVP/Hes did not affect the health of the mice. The pathological images of the organs and cornea (Fig. 8F) further confirmed the safety of the FU/PVP/Hes, without causing any pathological changes to the main organs of the mice.

4. Conclusion

The FU/PVP/Hes nanoparticle has been successfully synthesized and characterized, demonstrating excellent biocompatibility, antioxidant activity, and anti-inflammatory properties. *In vivo* studies have confirmed its therapeutic efficacy in promoting corneal epithelial healing and reducing corneal opacity in an alkali-induced corneal injury model. The nanoparticles' ability to suppress inflammatory cytokines and facilitate corneal tissue repair makes them a promising candidate for corneal injury treatment. Further studies and clinical trials are necessary to explore the full potential of this nanoparticle complex in ocular therapy.

Funding

This work was supported by Natural Science Foundation of Jiangsu Province (BK20241765), Shandong Provincial Natural Science Foundation (ZR2023ME045), Xuzhou Medical Key Talents Project (No. XWRCHT20220048), and Xuzhou Key R & D Program (No. KC22099).

CRediT authorship contribution statement

Yalu Liu: Writing – original draft, Visualization, Validation, Formal analysis, Data curation. **Zhengpei Zhang:** Writing – review & editing, Supervision. **Lina Guan:** Visualization, Validation, Formal analysis. **Jie Li:** Writing – original draft, Formal analysis. **Xing Ge:** Formal analysis, Data curation. **Xiaochen Wu:** Writing – review & editing, Supervision. **Haiyang Liu:** Writing – review & editing, Supervision, Funding acquisition.

Declaration of competing interest

The authors declare no competing financial interest.

Data availability

Data are available on request from the authors.

References

Adami, R., Di Capua, A., Reverchon, E., 2017. Supercritical assisted atomization for the production of curcumin-biopolymer microspheres. Powder Technol. 305, 455–461.

Barrientez, B., Nicholas, S.E., Whelchel, A., Sharif, R., Hjortdal, J., Karamichos, D., 2019. Corneal injury: clinical and molecular aspects. Exp. Eye Res. 186, 107709.

Cao, L.L., Wang, J.W., Zhang, Y.J., Tian, F., Wang, C.F., 2022. Osteoprotective effects of flavonoids: evidence from *in vivo* and *in vitro* studies. Mol. Med. Rep. 25, 200.

Cardoso, M.J., Costa, R.R., Mano, J.F., 2016. Marine origin polysaccharides in drug delivery systems. Mar. Drugs 14, 34.

Chen, Z., You, J., Liu, X., Cooper, S., Hodge, C., Sutton, G., Crook, J.M., Wallace, G.G., 2018. Biomaterials for corneal bioengineering. Biomed. Mater. 13, 032002.

Dang, D.H., Riaz, K.M., Karamichos, D., 2022. Treatment of non-infectious corneal injury: review of diagnostic agents, therapeutic medications, and future targets drugs, 82, 145–167.

Franco, P., De Marco, I., 2020. The Use of Poly(*N*-vinyl pyrrolidone) in the Delivery of Drugs: A Review Polymers, 12, p. 1114.

Ger, T.-Y., Yang, C.-J., Ghosh, S., Lai, J.-Y., 2023. Biofunctionalization of nanoceria with sperminated hyaluronan enhances drug delivery performance for corneal alkali burn therapy. Chem. Eng. J. 476, 146864.

Ger, T.-Y., Yang, C.-J., Bui, H.L., Lue, S.J., Yao, C.-H., Lai, J.-Y., 2025. Alginate-functionalized nanoceria as ion-responsive eye drop formulation to treat corneal abrasion. Carbohydr. Polym. 352, 123164.

Ghosh, S., Su, Y.-H., Yang, C.-J., Lai, J.-Y., 2025. Design of highly adhesive urchin-like gold nanostructures for effective topical drug administration and symptomatic relief of corneal dryness small structures, 6, 2400484.

Griffith, G.L., Kasus-Jacobi, A., Pereira, H.A., 2017. Bioactive antimicrobial peptides as therapeutics for corneal wounds and infections. Adv. Wound Care 6, 175–190.

Han, S.R.Y., Jeong, E., Cheon, S.Y., Lee, D.H.Y., Lee, Y., Lee, S.Y., Cho, H.J., Koo, H., 2022. Perfluorooctylbromide-loaded fucoidan-chlorin e6 nanoparticles for tumor-targeted photodynamic therapy. Int. J. Biol. Macromol. 223, 77–86.

Jian, H.-J., Wu, R.-S., Lin, T.-Y., Li, Y.-J., Lin, H.-J., Harroun, S.G., Lai, J.-Y., Huang, C.-C., 2017. Super-cationic carbon quantum dots synthesized from spermidine as an eye drop formulation for topical treatment of bacterial keratitis. ACS Nano 11, 6703–6716.

Jiang, H.H., Fei, X.Y., Zhang, G.W., Hu, X., Gong, D.M., Pan, J.H., 2023. Complexing with fibrillated glutenin and orange peel pectin improves the aqueous dispersion and storage stability of hesperitin/hesperidin. Food Hydrocoll. 145, 109138.

Kim, D.W., Lee, S.H., Shin, M.J., Kim, K., Ku, S.K., Youn, J.K., Cho, S.B., Park, J.H., Lee, C.H., Son, O., Sohn, E.J., Cho, S.-W., Park, J.H., Kim, H.A., Han, K.H., Park, J., Eum, W.S., Choi, S.Y., 2015. PEP-1-FK506BP inhibits alkali burn-induced corneal inflammation on the rat model of corneal alkali injury. BMB Rep. 48, 618–623.

Li, C.Y., Schluesener, H., 2017. Health-promoting effects of the citrus flavanone hesperidin. Crit. Rev. Food Sci. Nutr. 57, 613–631.

Liu, L.R., Chen, D., Sheng, S.T., Xu, J.W., Xu, W., 2023. Research progress on animal models of corneal epithelial-stromal injury. Int. J. Ophthalmol. 16, 1890–1898.

Luo, L.-J., Nguyen, D.D., Huang, C.-C., Lai, J.-Y., 2022. Therapeutic hydrogel sheets programmed with multistage drug delivery for effective treatment of corneal abrasion. Chem. Eng. J. 429, 132409.

Manju, S., Sreenivasan, K., 2011. Synthesis and characterization of a cytotoxic cationic polyvinylpyrrolidone-curcumin conjugate. J. Pharm. Sci. 100, 504–511.

Mikayilov, E., Tagiyev, D., Zeynalov, N., Tagiyev, S., 2024. Exploring the role of poly (N-vinyl pyrrolidone) in drug delivery. Chem. Biochem. Eng. Q. 38, 185–196.

Shen, C.L., Chen, R.N., Qian, Z.Y., Meng, X.M., Hu, T.T., Li, Y.Y., Chen, Z.L., Huang, C., Hu, C.J., Li, J., 2015. Intestinal absorption mechanisms of MTBH, a novel hesperetin derivative, in Caco-2 cells, and potential involvement of monocarboxylate transporter 1 and multidrug resistance protein 2. Eur. J. Pharm. Sci. 78, 214–224.

Simao, D.O., Honorato, T.D., Gobo, G.G., Piva, H.L., Goto, P.L., Rolim, L.A., Turrin, C.O., Blanzat, M., Tedesco, A.C., Siqueira-Moura, M.P., 2020. Preparation and cytotoxicity of lipid nanocarriers containing a hydrophobic flavanone. Coll. Surf. A Physicochem. Eng. Aspects 601, 124982.

Tran, K.N., Tran, P.H.L., Vo, T.V., Tran, T.T.D., 2016. Design of fucoidan functionalized - iron oxide nanoparticles for biomedical applications current. Drug Deliv. 13, 774–783.

Wang, H., Li, X., Yang, H., Wang, J., Li, Q., Qu, R., Wu, X., 2020. Nanocomplexes based polyvinylpyrrolidone K-17PF for ocular drug delivery of naringenin. Int. J. Pharmaceut. 578, 119133.

Yang, C.-J., Anand, A., Huang, C.-C., Lai, J.-Y., 2023a. Unveiling the power of gabapentin-loaded nanoceria with multiple therapeutic capabilities for the treatment of dry eye disease. ACS Nano 17, 25118–25135.

Yang, C.J., Nguyen, D.D., Lai, J.Y., 2023b. Poly(l-Histidine)-mediated on-demand therapeutic delivery of roughened ceria nanocages for treatment of chemical eye injury. Adv. Sci. (Weinh.) 10, e2302174.

Yin, L.F., Huang, S.J., Zhu, C.L., Zhang, S.H., Zhang, Q., Chen, X.J., Liu, Q.W., 2012. *In vitro* and *in vivo* studies on a novel solid dispersion of repaglinide using polyvinylpyrrolidone as the carrier. Drug Dev. Ind. Pharm. 38, 1371–1380.

Yin, C., Liu, Y., Qi, X., Guo, C., Wu, X., 2021a. Kaempferol incorporated bovine serum albumin fibrous films for ocular drug delivery. Macromol. Biosci. 21, 2100269.

Yin, C., Qi, X., Wu, J., Guo, C., Wu, X., 2021b. Therapeutic contact lenses fabricated by hyaluronic acid and silver incorporated bovine serum albumin porous films for the treatment of alkali-burned corneal wound. Int. J. Biol. Macromol. 184, 713–720.

Yu, F., Zhao, X., Wang, Q., Fang, P.H., Liu, L., Du, X.Y., Li, W.H., He, D.L., Zhang, T.T., Bai, Y., Liu, L., Li, S.Q., Yuan, J., 2024. Engineered mesenchymal stromal cell exosomes-loaded microneedles improve corneal healing after chemical injury. ACS Nano 18, 20065–20082.

Zahariev, N., Katsarov, P., Lukova, P., Pilicheva, B., 2023. Novel fucoidan pharmaceutical formulations and their potential application in oncology-a review polymers, 15, 3242.

Zhang, F., Li, R., Yan, M., Li, Q., Li, Y., Wu, X., 2020. Ultra-small nanocomplexes based on polyvinylpyrrolidone K-17PF: a potential nanoplatform for the ocular delivery of kaempferol. Eur. J. Pharm. Sci. 147, 105289.

Zhou, S.L., Sun, Y.X., Wang, K.D., Gao, X.T., Dong, K.H., Wang, J., Wu, X.C., Guo, C.L., 2024. Polyvinylpyrrolidone-Polydatin nanoparticles protect against oxaliplatin induced intestinal toxicity in vitro and in vivo. Food Chem. Toxicol. 184, 114427.